Available online at www.sciencedirect.com

SciVerse ScienceDirect

Ceramics International 38 (2012) 3619–3624

CERAMICS INTERNATIONAL

www.elsevier.com/locate/ceramint

# Effects of mechanical milling on preparation and properties of $CuAl_{1-x}Fe_xO_2$ thermoelectric ceramics

Yi-Cheng Liou [a,b], Li-Shin Chang [c], Yang-Ming Lu [d,*], Hong-Chou Tsai [e], Uang-Ru Lee [a]

[a] Department of Electronic Engineering, Kun Shan University, Tainan 71003, Taiwan, ROC
[b] Nano Technology Research and Development Center, Kun Shan University, Taiwan, ROC
[c] Department of Materials Science and Engineering, National Chung Hsing University, Taichung 402, Taiwan, ROC
[d] Department of Electrical Engineering, National University of Tainan, 33, Sec. 2, Shu-Lin St., Tainan 700, Taiwan, ROC
[e] Master Program of Electro-Optical Engineering, Department of Electrical Engineering, National University of Tainan, Tainan 700, Taiwan, ROC

Received 6 August 2011; received in revised form 30 December 2011; accepted 30 December 2011
Available online 9 January 2012

**Abstract**

$CuAl_{1-x}Fe_xO_2$ ($x = 0$, 0.1, and 0.2) thermoelectric ceramics produced by a reaction-sintering process were investigated. Pure $CuAlO_2$ and $CuAl_{0.9}Fe_{0.1}O_2$ were obtained. Minor $CuAl_2O_4$ phase formed in $CuAl_{0.8}Fe_{0.2}O_2$. Addition of 10 mol% Fe lowered the sintering temperature obviously and enhanced the grain growth. At $x = 0.1$, electrical conductivity = 3.143 $\Omega^{-1}$ $cm^{-1}$, Seebeck coefficient = 418 $\mu V$ $K^{-1}$, and power factor = $5.49 \times 10^{-5}$ W $m^{-1}$ $K^{-2}$ at 600 °C were obtained. The reaction-sintering process is simple and effective in preparing $CuAlO_2$ and $CuAl_{0.9}Fe_{0.1}O_2$ thermoelectric ceramics for applications at high temperatures.
© 2012 Elsevier Ltd and Techna Group S.r.l. All rights reserved.

*Keywords:* $CuAl_{1-x}Fe_xO_2$; Thermoelectric; Mechanical milling

## 1. Introduction

Thermoelectric materials can directly convert a gradient of temperature into electrical current and vice versa. Oxide systems such as $In_2O_3$–$MO_x$ (M = Cr, Mn, Ni, Zn, Y, Nb, and Sn) [1], (Ca, Ln)$MnO_3$ [2], (Zn, Al)O [3], (Ba, Sr)$PbO_3$ [4], and $(ZnO)_5In_2O_3$ [5] have been investigated for thermoelectric application. The figure of merit $Z = S^2\sigma/\kappa$ is often used to evaluate the performance of thermoelectric materials. $S$, $\sigma$, and $\kappa$ are the Seebeck coefficient, electrical conductivity, and thermal conductivity, respectively. The figure of merit $Z$ for the above systems is lower than $Z$ for alloys and semiconductors [6]. A high figure of merit $8.8 \times 10^{-4}$ $K^{-1}$ in $NaCo_2O_4$ was reported. However, its application is limited due to the volatility of sodium above 800 °C and the hygroscopicity in air [7]. $Ca_3Co_4O_{9+\delta}$ ($\delta = 0.33$) was first synthesized in 1968 [8], and Woermann grew the single crystal of $Ca_3Co_4O_9$ later in 1970 [9]. Shikano and Funahashi prepared single crystals $Ca_3Co_4O_9$ with a high thermoelectric figure of merit ZT ~ 0.87 at 700 °C. This makes $Ca_3Co_4O_9$ a promising material for practical application in thermoelectric power generation [10]. Recently, $CuAlO_2$ had received many attentions. Ishiguro et al. extensively studied the crystalline structure of $CuAlO_2$ [11]. Koumoto et al. first reported delafossite $CuAlO_2$ with a power factor ~ $1.04 \times 10^{-4}$ W $m^{-1}$ $K^{-2}$ for single crystal and a power factor ~ $2.0 \times 10^{-5}$ W $m^{-1}$ $K^{-2}$ for polycrystalline at 1073 K [12]. Park et al. obtained power factors $4.98 \times 10^{-5}$ and $6.62 \times 10^{-5}$ W $m^{-1}$ $K^{-2}$ (at 1140 K) for the $CuAlO_2$ ceramics sintered at 1433 and 1473 K, respectively [13]. They also found the substitution of Ca for Al in the $CuAl_{1-x}Ca_xO_2$ samples gave rise to an increase in both $\sigma$ and $S$ (up to $x = 0.1$). On the other hand, the higher Ca substitution ($x \geq 0.15$) decreased both $\sigma$ and $S$. The highest value of power factor $7.82 \times 10^{-5}$ W $m^{-1}$ $K^{-2}$ was attained for $CuAl_{0.9}Ca_{0.1}O_2$ at 1140 K [14]. Park et al. reported $\sigma$ increased with Fe addition up to $x = 0.1$ in $CuAl_{1-x}Fe_xO_2$ ($0 \leq x \leq 0.2$) due to the increase of grain size, density, and carrier density. Fe addition up to $x = 0.1$ caused a decrease in the Seebeck coefficient due to an increase of carrier density. The highest value of power factor $1.1 \times 10^{-4}$ W $m^{-1}$ $K^{-2}$ was attained for $CuAl_{0.9}Fe_{0.1}O_2$ at

* Corresponding author. Tel.: +886 6 2606123; fax: +886 6 2602305.
*E-mail address:* ymlumit@yahoo.com.tw (Y.-M. Lu).

0272-8842/$36.00 © 2012 Elsevier Ltd and Techna Group S.r.l. All rights reserved.
doi:10.1016/j.ceramint.2011.12.079

1140 K [15]. Therefore, $CuAlO_2$ based ceramics are promising thermoelectric materials for energy conversion. Various methods had been used to prepare $CuAlO_2$ based ceramics, including the conventional solid-state reaction [13–15], ion exchange [16], and sol–gel process [17].

We used a simple and effective non-calcining process, i.e. reaction-sintering process, in preparing $Pb(Mg_{1/3}Nb_{2/3})O_3$ (PMN) ceramics years ago. A mixture of raw materials was sintered into PMN ceramics by bypassing calcination and subsequent pulverization stages. These have been the first successful synthesis of perovskite relaxor ferroelectric ceramics without involving the calcinations step in the conventional solid-state reaction route. Highly dense PMN ceramics with a density 8.09 g/cm$^3$ (99.5% of the theoretical value) and high dielectric constant 19,900 (at 1 kHz) were obtained [18]. Reaction-sintering process had also been used to produce other complex perovskite relaxor ceramics. In recent studies, we also prepared microwave dielectric ceramics such as $BaTi_4O_9$, $Ba_5Nb_4O_{15}$, $Sr_5Nb_4O_{15}$, and $NiNb_2O_6$ using reaction-sintering process [19–21]. In this study, we try to obtain $CuAl_{1-x}Fe_xO_2$ ($x = 0$, 0.1, and 0.2) thermoelectric ceramics via the reaction-sintering process.

## 2. Experimental procedures

$CuAlO_2$ (CA), $CuAl_{0.9}Fe_{0.1}O_2$ (CAF1), and $CuAl_{0.8}Fe_{0.2}O_2$ (CAF2) ceramics in this study were prepared from reagent-grade powders: CuO (99%, SHOWA, Japan), $Al_2O_3$ (99.5%, SHOWA, Japan), and $Fe_2O_3$ (100%, J.T. Baker, USA). Appropriate amounts of raw materials were weighed and put into a PE (polyethylene) bottle. Zirconia balls (weight ratio: balls/powders = 2.85) with 5 and 10 mm diameters were used for milling the raw mother powders with de-ionized water (weight ratio: water/powders = 3.75) for 12 h at a speed of 500 rpm. The milled and non-milled powders were analyzed by X-ray diffraction (XRD) to understand the effects of mechanical milling. Results indicated that only peaks for raw mother powders were detected. The dried and pulverized powders of mixtures were pressed into pellets with 12 mm in diameter and 1–2 mm thick. The pellets were sintered at 1050–1350 °C for 2 h at a rate 10 °C/min in a covered alumina crucible in air.

We analyzed the sintered pellets by XRD to identify the reflections of various phases. Microstructures were analyzed by scanning electron microscopy (SEM). The density of the sintered pellets was measured using the Archimedes method. The standard four-probe technique was used for electrical resistivity measurements at temperatures ranging from 25 to 600 °C. A Keithley 2182A nanovoltmeter was used to measure the thermally generated Seebeck voltage across the sample.

## 3. Results and discussion

To check phases formed in CA at various temperatures, green pellets were heated to 600–1100 °C and then cooled immediately. There were only CuO and $Al_2O_3$ detected for pellets heated to 600–1000 °C as shown in Fig. 1. $CuAlO_2$ and $CaAl_2O_4$ were detected in pellets heated to 1100 °C indicating

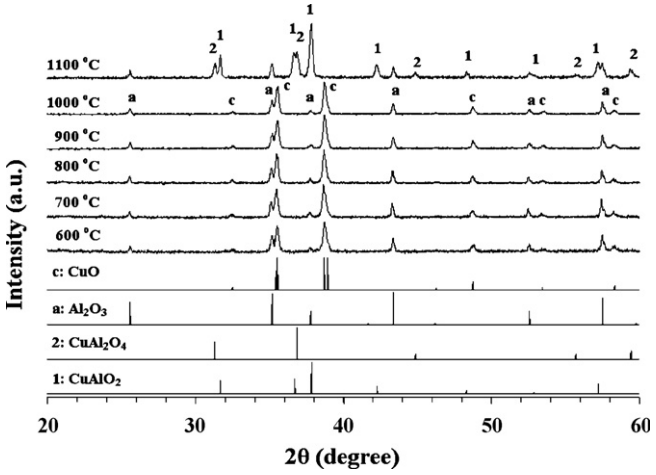


Fig. 1. XRD patterns of CA green pellets heated to 600–1100 °C and then cooled immediately. $CuAlO_2$: ICDD PDF # 00-035-1401, $CuAl_2O_4$: ICDD PDF # 00-033-0448, CuO: ICDD PDF # 00-001-1117, and $Al_2O_3$: ICDD PDF # 00-042-1468.

the reaction of the raw materials occurred between 1000 °C and 1100 °C. This result is consistent to the study reported by Park and co-workers. They reported the reaction of CuO and $Al_2O_3$ occurred at 1069–1095 °C [13]. Tonooka et al. [22] reported that $CuAl_2O_4$ formed as a reaction intermediate and reacted with CuO to form $CuAlO_2$ at approximately 1050 °C by a nitrate process. The reaction of the raw materials occurred at the heating up period and the calcination stage in the conventional solid-state reaction was bypassed in this study. The XRD profiles for sintered CA, CAF1, and CAF2 are illustrated in Fig. 2. The reflections match well with those of $CuAlO_2$ in ICDD PDF # 00-035-1401 and no secondary phase detected in CA and CAF1. This implies that 1200 °C is high enough for a complete reaction among mixed raw materials and a solid solution was formed. Park et al. reported an endothermic reaction occurs at 1069–1095 °C for the mixed powders of $CuAlO_2$ and at 1051–1086 °C for the mixed powders of $CuAl_{0.8}Fe_{0.2}O_2$ [15]. The reaction-sintering process is proven a simple and effective process to obtain CA and CAF1 ceramics. In our previous study of $CuAl_{0.9}Ca_{0.1}O_2$ ceramics prepared via the reaction-sintering process, $CaAl_4O_7$ and CuO were detected

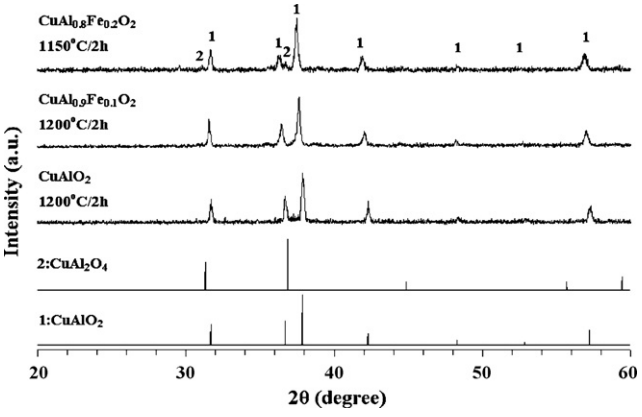


Fig. 2. XRD patterns of sintered CA, CAF1, and CAF2 ceramics.

[23]. 10 mol% Fe seemed to be more effective than 10 mol% Ca in eliminating the secondary phases in CA ceramics. While in CAF2, weak reflections appeared around $2\theta = 31^\circ$ and $2\theta = 37^\circ$ indicating the formation of minor $CuAl_2O_4$ phase. Park et al. observed a small amount of non-reacted CuO detected in CA ceramics. Secondary phases CuO, $Fe_2O_3$, and $CuFeO_2$ were found in CAF1 and CAF2 ceramics after calcining the mixed powders at 800 °C/2 h and sintered twice at 1200 °C/20 h (crushed and milled after the first sintering) [15]. In this study, single phase CA and CAF1 ceramics were obtained after sintering at 1200 °C/2 h without involving any calcination stage. Therefore, the reaction-sintering process is proven more effective than the conventional solid-state reaction method in preparing single phase CA and CAF1 ceramics.

Density of CA, CAF1, and CAF2 ceramics sintered at various temperatures for 2 h is shown in Fig. 3. Low density 3.01 g/cm$^3$ was found for CA pellets sintered at 1200 °C indicating a poor densification. It increased linearly with the sintering temperature and reached 3.66 g/cm$^3$, 71.81% of the theoretical density 5.097 g/cm$^3$, after 1350 °C sintering. For CAF1, addition of 10 mol% Fe lowered the sintering temperature obviously. Dense pellets of 4.6 g/cm$^3$, 90.25% of the theoretical density 5.097 g/cm$^3$ of $CuAlO_2$, were observed after 1200 °C sintering. CAF2 pellets of 4.46 g/cm$^3$ were observed after 1100 °C sintering. Therefore, the sintering temperature for CA ceramics could be lowered by the addition of Fe. After calcining at 800 °C/2 h and sintering twice at 1200 °C/20 h, Park et al. [15] reported 85.2% and 89.9% of the theoretical density in CAF1 and CAF2, respectively. The reaction-sintering process is proven more effective than the conventional solid-state reaction method in preparing dense CAF1 and CAF2 ceramics.

SEM photographs of as-sintered CA, CAF1, and CAF2 ceramics after sintering at 1200 °C/2 h are presented in Fig. 4. 1200 °C is not high enough for grain growth in CA and large amount of pores formed. Grains larger than 20 μm were seen in CAF1 sintered at 1200 °C indicating addition of 10 mol% Fe lowered the sintering temperature obviously and enhanced the grain growth. Grains less than 8 μm were seen in CAF2 sintered at 1200 °C. The smaller grain size in CAF2 was thought to be caused by the formation of $CuAl_2O_4$, which inhibited the grain growth of CAF2. Wongcharoen et al. observed grain growth of Ni-doped $CuAlO_2$ was reduced by the formation of CuO and $CuAl_2O_4$. They found grain size decreased from 6 to 2 μm when $x$ increased from 0 to 0.1 in $CuAl_{1-x}Ni_xO_2$ [24]. After calcining at 800 °C/2 h and sintering twice at 1200 °C/20 h, Park et al. obtained average grain size of 2.08 μm (distributed in ~1–5 μm) and 2.7 μm (distributed in ~1–6 μm) in CAF1 and CAF2, respectively [15]. Therefore, the reaction-sintering process is proven more effective than the conventional solid-state reaction method for grain growth in CAF1 and CAF2. The major difference between the reaction-sintering process and the conventional solid-state reaction method is that the mixed raw materials were pressed and

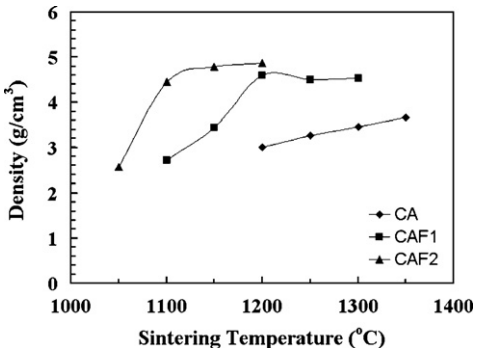


Fig. 3. Density of CA, CAF1, and CAF2 ceramics sintered at various temperatures for 2 h.

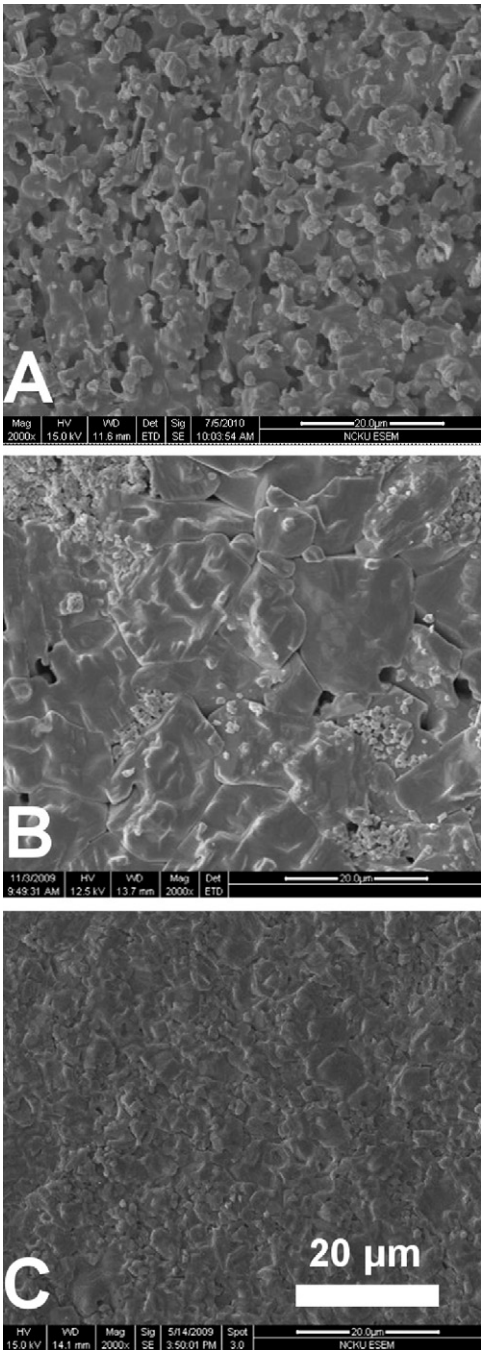


Fig. 4. SEM photographs of as-fired (A) CA, (B) CAF1, and (C) CAF2 ceramics sintered at 1200 °C for 2 h.

sintered directly in the reaction-sintering process. The calcination stage and the following pulverization were bypassed. The clusters of calcined powder via the conventional solid-state reaction did not exist in the pressed pellets of mixed raw materials via the reaction-sintering process. Sizes for clusters of calcined powder are larger than particles in the milled mixed raw materials without calcining. The driving force to break the contact surface of calcined clusters is higher. While the driving force to join the reacted and nucleated small particles in the pressed pellets containing mixed raw materials is lower. On the other hand, CuO is often used as a sintering aid to lower the sintering temperature in preparing ceramics. The sintering temperature was 200 °C lowered in $Ba_5Nb_4O_{15}$ ceramics with the addition of 1 wt% CuO via the reaction-sintering process [20]. Yang et al. [25] used the CuO–BaO mixture as a sintering aid in the fabrication of $BaTiO_3$ ceramics and studied its effects on the microstructure and densities of $BaTiO_3$ ceramics. An addition of 1 wt% CuO–BaO mixture significantly increased the sintering rate of $BaTiO_3$ at a temperature between 1000 and 1100 °C. In this study, some parts of mixed raw materials in the pressed green pellets reacted into CAF1 or CAF2 first and then nucleated and grew to larger grains. It was possible that these firstly formed CAF1 or CAF2 grains were surrounded by CuO particles and a liquid phase sintering occurred at the heating period. Therefore, the reaction of raw materials and a liquid phase sintering were supposed to occur at the same period. This may be the reason why larger grains formed in CAF1 and CAF2 via the reaction-sintering process. While in CA, the reaction for $CuAlO_2$ formation and nucleation occurred at a higher temperature 1069–1095 °C. Most CuO reacted with $Al_2O_3$ before the grain growth began. Therefore, less CuO remained to form liquid phase during the grain growth in CA and resulted in smaller grains.

$\sigma$ of CA, CAF1, and CAF2 ceramics sintered at 1200 °C for 2 h is shown in Fig. 5. $\sigma$ of CA was 0.021 $\Omega^{-1}$ cm$^{-1}$ at 25 °C and increased to 1.815 $\Omega^{-1}$ cm$^{-1}$ at 600 °C. Park et al. obtained ~1.8 $\Omega^{-1}$ cm$^{-1}$ at 600 °C for CA after calcining at 800 °C/2 h and sintering twice at 1200 °C/20 h [15]. $\sigma$ of CAF1 was 3.143 $\Omega^{-1}$ cm$^{-1}$ at 600 °C in Fig. 5. Park et al. reported that the addition of Fe up to 10 mol% increased $\sigma$ at 600 °C to ~4.4 $\Omega^{-1}$ cm$^{-1}$ for CAF1 [15]. It should be noted, phases formed in their CAF1 pellets and the CAF1 pellets in this study are different. Park et al. observed secondary phases CuO, $Fe_2O_3$, and $CuFeO_2$ in CAF1. Ruttanapun et al. reported 3.5 $\Omega^{-1}$ cm$^{-1}$ at 27 °C and ~11 $\Omega^{-1}$ cm$^{-1}$ at 600 °C for $\sigma$ of $CuFeO_2$ [26]. As no $CuFeO_2$ was detected in this study, a lower $\sigma$ of CAF1 is reasonable. Also in Fig. 5, $\sigma$ of CAF2 was obviously lower than $\sigma$ of CA and CAF1, especially at 200–600 °C. The formation of $CuAl_2O_4$ phase was thought to be the major reason. A similar result was also observed in CAF2 by Park et al. and they thought the major reason is the increased amount of $Fe_2O_3$ with quite low $\sigma$ [15]. Another possible reason was the n-type doping due to the $Fe^{2+}$ (ionic radius = 0.074 nm) substituted into $Cu^+$ (ionic radius = 0.095 nm) site. This would cause a decrease of hole concentration and resulted in a lower $\sigma$. Wongcharoen et al. reported that the substitution of $Ni^{2+}$ (ionic radius = 0.069 nm) in $Cu^+$ site may decrease the hole concentration leading to an increase in the electrical resistivity in $CuAl_{1-x}Ni_xO_2$ samples [24].

$S$ of CA, CAF1, and CAF2 ceramics sintered at 1200 °C for 2 h is shown in Fig. 6. Positive values indicated that the major conductivity carriers were holes and p-type thermoelectric ceramics were obtained. For CA, $S$ = 513 μV K$^{-1}$ was found at 25 °C and it decreased to a minimum 237 μV K$^{-1}$ at 500 °C then increased to 456 μV K$^{-1}$ at 600 °C. Similar trend was observed by Park et al. [15] and a minimum $S$ ~ 480 μV K$^{-1}$ occurred at 400 °C then increased at higher temperatures. For CAF1 in Fig. 6, a minimum $S$ = 315 μV K$^{-1}$ at 300 °C was observed and it increased to 418 μV K$^{-1}$ at 600 °C. The shift of temperature for minimum $S$ was not observed by Park et al. [15]. A minimum $S$ ~ 400 μV K$^{-1}$ was measured for CAF1 at 400 °C, the same temperature for CA. This is again resulted from the different phase formation in CAF1 for their study and this study. It is well known that $S$ usually decreases with increasing carrier concentration (leading to the increase of electrical conductivity) in semiconductor materials [27,28]. However, $S$ of CA was lower than $S$ of CAF1 at 400 °C and 500 °C in Fig. 6. Yanagiya et al. observed $\sigma$ and $S$ of $Cu_{0.979}Ag_{0.02}Zn_{0.001}AlO_2$ at temperature above 1000 K were higher than $\sigma$ and $S$ of CA. They thought such phenomena cannot be explained by the above-mentioned general relationship between $\sigma$ and $S$. The energy correlated carrier mobility

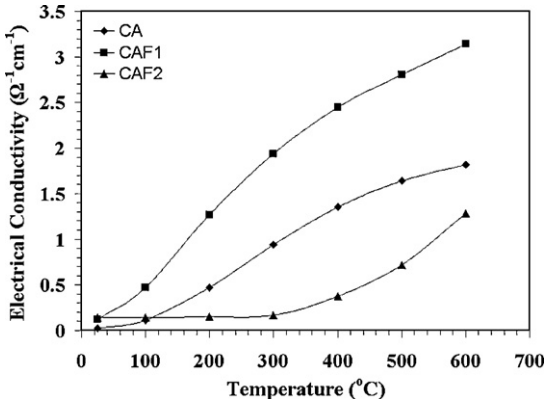


Fig. 5. Electrical conductivity for CA, CAF1, and CAF2 ceramics sintered at 1200 °C for 2 h.

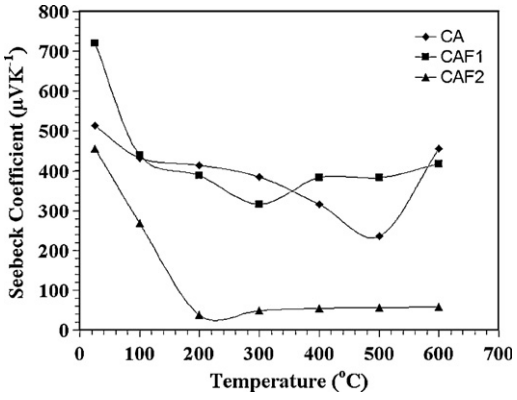


Fig. 6. Seebeck coefficient for CA, CAF1, and CAF2 ceramics sintered at 1200 °C for 2 h.

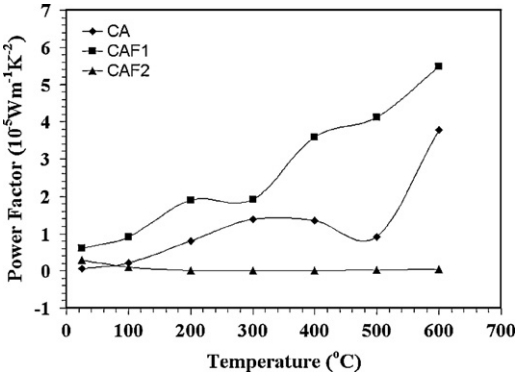


Fig. 7. Power factor for CA, CAF1, and CAF2 ceramics sintered at 1200 °C for 2 h.

$\mu(E)$ may play a crucial role in determining $S$. They assumed that addition of Ag and Zn has changed $\mu(E)$, and the change of the $\mu(E)$ affects the increase of $S$ [27]. We thought this may be the reason why $S$ of CA was lower than $S$ of CAF1 at 400 °C and 500 °C in Fig. 6. $S$ of CAF2 in Fig. 6 was obviously lower than CA and CAF1, especially at 200–600 °C. The formation of $CuAl_2O_4$ phase was thought to be the major reason. A quite different result was observed in CAF2 reported by Park and co-workers. $S$ of CAF2 was higher than $S$ for CA and CAF1, and a minimum $S \sim 490\ \mu V\ K^{-1}$ at 500 °C was observed. They thought the major reason was the increased amount of $Fe_2O_3$ with a large $S$ [15].

Power factor of CA, CAF1, and CAF2 ceramics sintered at 1200 °C for 2 h is shown in Fig. 7. Values less than $2 \times 10^{-5}\ W\ m^{-1}\ K^{-2}$ were measured except CA at 600 °C and CAF1 at 400–600 °C. $3.78 \times 10^{-5}\ W\ m^{-1}\ K^{-2}$ at 600 °C was found for CA and $5.49 \times 10^{-5}\ W\ m^{-1}\ K^{-2}$ at 600 °C was found for CAF1. Poor power factor less than $2.9 \times 10^{-6}\ W\ m^{-1}\ K^{-2}$ was obtained for CAF2 ceramics due to low $\sigma$ and low $S$ caused by the $CuAl_2O_4$ phase. Park et al. obtained power factor $\sim 3.5 \times 10^{-5}\ W\ m^{-1}\ K^{-2}$ for CA and power factor $\sim 8.2 \times 10^{-5}\ W\ m^{-1}\ K^{-2}$ for CAF1 at 600 °C after calcining at 800 °C/2 h and sintering twice at 1200 °C/20 h [15]. Therefore, the reaction-sintering process is proven as effective as the conventional solid-state reaction method in preparing CA ceramics with similar power factor. Addition of 10 mol% Fe into CA effectively enhanced the high-temperature thermoelectric properties.

## 4. Conclusions

Pure $CuAlO_2$ and $CuAl_{0.9}Fe_{0.1}O_2$ were obtained by a reaction-sintering process with the calcinations and subsequent pulverization stages bypassed. While in $CuAl_{0.8}Fe_{0.2}O_2$, the formation of minor $CuAl_2O_4$ phase was observed. Addition of 10 mol% Fe lowered the sintering temperature obviously and enhanced the grain growth. Grains larger than 20 μm were seen in $CuAl_{0.9}Fe_{0.1}O_2$ pellets sintered at 1200 °C. Electrical conductivity of $3.143\ \Omega^{-1}\ cm^{-1}$, Seebeck coefficient of $418\ \mu V\ K^{-1}$, and power factor of $5.49 \times 10^{-5}\ W\ m^{-1}\ K^{-2}$ at 600 °C were obtained for $CuAl_{0.9}Fe_{0.1}O_2$. The reaction-sintering process is simple and effective to prepare $CuAlO_2$ and $CuAl_{0.9}Fe_{0.1}O_2$ thermoelectric ceramics for applications at high temperatures.

## References

[1] M. Ohtaki, D. Ogura, K. Eguchi, H. Arai, High-temperature thermoelectric properties of $In_2O_3$-based mixed oxides and their applicability to thermoelectric-power generation, J. Mater. Chem. 4 (1994) 653–656.
[2] M. Ohtaki, D. Ogura, K. Eguchi, H. Arai, Electrical transport properties and high temperature thermoelectric performance of $(Ca_{0.9}M_{0.1})MnO_3$, J. Solid State Chem. 120 (1995) 105–111.
[3] M. Ohtaki, D. Ogura, K. Eguchi, H. Arai, High-temperature thermoelectric properties of $(Zn_{1-x}Al_x)O$, J. Appl. Phys. 79 (1996) 1816–1818.
[4] M. Yasukawa, N. Murayama, High temperature thermoelectric properties of $Ba_{1-x}Sr_xPbO_3$, J. Mater. Sci. Lett. 16 (1997) 1731–1734.
[5] M. KazeoKa, H. Hiramatsu, W. Seo, K. Koumoto, Improvement in the thermoelectric properties of $(ZnO)_5In_2O_3$ through partial substitution of yttrium for indium, J. Mater. Res. 13 (1998) 523–526.
[6] T. Kobayashi, H. Takizawa, T. Endo, T. Sato, M. Shimada, Metal-insulator transition and thermoelectric properties in the system $(R_{1-x}Ca_x)MnO_3$, (R: Tb, Ho, Y), J. Solid State Chem. 92 (1) (1991) 116–129.
[7] T. Itoh, T. Kawata, T. Kitajima, I. Terasaki, Large thermoelectric power in $NaCo_2O_4$ single crystals, Phys. Rev. B 56 (1997) 12685–12687.
[8] JCPDS Card, 21-139.
[9] E. Wocermann, A. Muan, Phase equilibria in the system CaO-cobalt oxide in air, J. Inorg. Nucl. Chem. 32 (5) (1970) 1455–1459.
[10] M. Shikano, R. Funahashi, Electrical and thermal properties of single-crystalline $(Ca_2CoO_3)_{0.7}CoO_2$ with a $Ca_3Co_4O_9$ structure, Appl. Phys. Lett. 82 (12) (2003) 1851–1853.
[11] T. Ishiguro, A. Kitazawa, N. Mizutani, M. Kato, Single-crystal growth and crystal structure refinement of $CuAlO_2$, J. Solid State Chem. 40 (2) (1981) 170–174.
[12] K. Koumoto, H. Koduka, W.S. Seo, Thermoelectric properties of single crystal $CuAlO_2$ with a layered structure, J. Mater. Chem. 11 (2001) 251–252.
[13] K. Park, K.Y. Ko, W.S. Seo, Thermoelectric properties of $CuAlO_2$, J. Eur. Ceram. Soc. 25 (2005) 2219–2222.
[14] K. Park, K.Y. Ko, W.S. Seo, Effect of partial substitution of Ca for Al on the microstructure and high-temperature thermoelectric properties of $CuAlO_2$, Mater. Sci. Eng. B 129 (2006) 1–7.
[15] K. Park, K.Y. Ko, H.-C. Kwon, S. Nahm, Improvement in thermoelectric properties of $CuAlO_2$ by adding $Fe_2O_3$, J. Alloys Compd. 437 (2007) 1–6.
[16] Th. Dittrich, L. Dloczik, T. Guminskaya, M.Ch. Lux-Steiner, N. Grigorieva, I. Urban, Photovoltage characterization of $CuAlO_2$ crystallites, Appl. Phys. Lett. 85 (5) (2004) 742–744.
[17] Z. Deng, X. Zhu, R. Tao, W. Dong, X. Fang, Synthesis of $CuAlO_2$ ceramics using sol–gel, Mater. Lett. 61 (2007) 686–689.
[18] Y.C. Liou, K.H. Tseng, Stoichiometric $Pb(Mg_{1/3}Nb_{2/3})O_3$ perovskite ceramics produced by reaction-sintering process, Mater. Res. Bull. 38 (8) (2003) 1351–1357.
[19] Y.C. Liou, C.T. Wu, K.H. Tseng, T.C. Chung, Synthesis of $BaTi_4O_9$ ceramics by reaction-sintering process, Mater. Res. Bull. 40 (9) (2005) 1483–1489.
[20] Y.C. Liou, W.H. Shiu, C.Y. Shih, Microwave ceramics $Ba_5Nb_4O_{15}$ and $Sr_5Nb_4O_{15}$ prepared by a reaction-sintering process, Mater. Sci. Eng. B 131 (2006) 142–146.
[21] Y.C. Liou, C.Y. Shiue, M.H. Weng, Synthesis and properties of $TiO_2$ added $NiNb_2O_6$ microwave dielectric ceramics using a simple process, J. Eur. Ceram. Soc. 29 (6) (2009) 1165–1171.
[22] K. Tonooka, K. Shimokawa, O. Nishimura, Properties of copper–aluminum oxide films prepared by solution methods, Thin Solid Films 411 (2002) 129–133.
[23] Y.C. Liou, U.R. Lee, Non-calcining process for $CuAlO_2$ and $CuAl_{0.9}Ca_{0.1}O_2$ ceramics, J. Alloys Compd. 467 (1–2) (2009) 496–500.
[24] N. Wongcharoen, T. Gaewdang, Thermoelectric properties of Ni-doped $CuAlO_2$, Phys. Procedia 2 (2009) 101–106.

[25] C.F. Yang, L. Wu, T.S. Wu, A new sintering agent for $BaTiO_3$: the binary BaO–CuO systems, J. Mater. Sci. Lett. 11 (18) (1992) 1246–1248.

[26] C. Ruttanapun, A. Wichainchai, W. Prachamon, A. Yangthaisong, A. Charoenphakdee, T. Seetawan, Thermoelectric properties of $Cu_{1-x}Pt_xFeO_2$ ($0.0 \leq x \leq 0.05$) delafossite-type transition oxide, J. Alloys Compd. 509 (2011) 4588–4594.

[27] S. Yanagiya, N.V. Nong, J. Xu, N. Pryds, The effect of (Ag, Ni, Zn)-addition on the thermoelectric properties of copper aluminate, Materials 3 (2010) 318–328.

[28] D.M. Rowe, General principles and basic considerations, in: D.M. Rowe (Ed.), Thermoelectrics Handbook: Macro to Nano, CRC Press, Boca Raton, FL, USA, 2006, p. 1.